DOI 10.1007/s11055-024-01574-1
Neuroscience and Behavioral Physiology, Vol. 54, No. 1, January, 2024

Physiology of Higher Nervous (Cognitive) Activity in Humans

Spatiotemporal Patterns of Corticomuscular Interactions in Locomotion

S. A. Moiseev and R. M. Gorodnichev

UDC 612.463:612.743

Translated from Zhurnal Vysshei Nervnoi Deyatel'nosti imeni I. P. Pavlova, Vol. 73, No. 5, pp. 666–679, September–October, 2023. Original article submitted November 7, 2022. Accepted July 3, 2023.

This study addressed the synergistic effects apparent at the cortical and muscular levels during locomotor activity performed under conditions in which the lower limbs are supported horizontally. The spatiotemporal structure of synergies was studied using data matrix factorization methods. Control of movement structure is shown to be realized primarily through three muscle synergies. Synchronization of the activity of the motor, associative, visual, and sensorimotor areas of the cortex on both sides is due to the specific characteristics of locomotion in conditions of gravitational unloading and the associated features of receptor signaling. The components identified, evidencing synchronization of different areas of the cortex on the right and left sides, may reflect control processes associated with the control of alternating activation of the flexor and extensor muscles of the contralateral limb in the process of locomotion. Data on the spatiotemporal structuring of cortical activity indicate separate control of muscle synergies via synchronization of cortical commands and the temporal organization of muscle synergies in the frequency range 0.30–8.00 Hz. These patterns may reflect operation of a rhythm-generating mechanism involved in controlling cyclic activity.

Keywords: muscle synergies, cortical control of locomotion, corticomuscular interaction.

Introduction. One concept in motor control is that the human motor system is organized in such a way that its elements combine to form modules of lower dimensionality, i.e., synergy [Bernstein, 1990; Latash, 2010]. Such an organization is designed to exert more effective control over the multiple elements of the system being controlled and to ensure stability of the discrete or cyclic motor actions being performed. Patterns of interaction between the elements of the controlled systems characteristic of synergy are found at different levels of examination of synergistic effects, though the field addressing interactions between the cortical and muscular levels remains less studied.

An effective approach to studying the role of central nervous system structures in generating synergies consists of stimulating brain structures and recording measures of motor output at the muscle level. For example, spatial patterns of muscle synergies could be correlated with stimulating electrode locations [Amundsen et al., 2017]. Responses from arm muscles evoked by transcranial magnetic stimulation (TMS) have been shown to have a similar modular structure to voluntary movements [Yarossi et al., 2022]. In addition, TMS-based evidence has shown that the hand movements induced by this stimulation are formed on the basis of natural (fundamental) synergistic muscle modules, with the motor cortex being the main area for controlling the structure of finger movements [Pei et al., 2022]. In addition to TMS, electrical stimulation of the spinal cord is used to study synergistic effects [Gerasimenko et al., 2015; Moiseev, 2022]. Applied at the levels of the T11–T12 and L1–L2 vertebrae, TMS helps maintain a vertical posture and can initiate involuntary stepping movements, similar in kinematic structure and the nature of intermuscular interaction to voluntary locomotion. It is probable that cortical commands influence spinal stepping movement generator, thereby generating modulated signals determining the spatiotemporal structuring of intermuscular interactions. However, there is a view that cortical activity is a "binding" signal, not a modulatory one, and such binding does not contribute to individual control, but exclusively to synergistic control [Reyes et al., 2017; Frère et al., 2017].

Velikie Luki State Academy for Physical Culture and Sport, Velikie Luki, Russia; e-mail: sergey_moiseev@vlgafc.ru.

In addition, studies have shown that muscle activity can be controlled via two independent mechanisms, including, in the first case, control of individual muscles through direct corticospinal projections, and in the second, by influencing muscle groups that function in synergy. Evidence for these comes from investigation of intermuscular and cortical interactions in the frequency domain [DeVries et al., 2016; Zandvoort et al., 2019; Yokoyama et al., 2019].

The intramuscular and intra-articular receptor systems play an important role in maintaining vertical posture and locomotion; a special role belongs to afferentation from the supporting surfaces of the foot [Grigoriev et al., 2004]. These signals modulate locomotor synergy patterns generated by spinal neural structures, which can lead to the emergence of "combined" temporal profiles of muscle activation with multiple peaks in different phases of the locomotor cycle [Hug et al., 2011]. However, despite a significant number of studies, the role of cortical structures in the formation of synergistic interlimb patterns remains largely unclear. Performance of step-like movements while lying on the side with the lower limbs hanging creates the need to control movement structure consciously, such that the roles of cortical and supraspinal influences on the structure of locomotion may increase. The involvement of the spinal stepping movements generator in forming locomotor patterns will probably be reduced, because of the specificity of afferent information in such conditions. It seems appropriate to use such a motor model to identify cortical commands influencing the organization of muscle synergies. The aim of the present work was to study the synergistic effects which become apparent at the cortical and muscular levels during locomotor activity performed with the lower limbs supported horizontally. Synergistic effects were understood as combined changes in movement characteristics as identified by data factorization methods. The study proceeded from the supposition that muscle synergies are controlled by descending cortical signals which modulate the main characteristics of the spatiotemporal interaction of the skeletal muscles involved in implementation of the bilateral stepping cycle.

Methods. A total of eight healthy male subjects aged 21–26 years took part in the studies. Experiments were carried out at the Velikie Luki State Academy for Physical Culture and Sport. All studies were conducted in compliance with the requirements and principles of biomedical ethics formulated in the 1964 Declaration of Helsinki and were approved by the local Bioethics Committee. Each participant provided voluntary written informed consent to participate in the research.

Subjects were placed in a lower limb horizontal support device [Gurfinkel et al., 1998; Gorodnichev et al., 2012]. The research protocol included performing voluntary locomotion at a free pace. A minimum of eight complete stride cycles were included in the analysis. In conditions of horizontal elevation of the lower limbs, the boundary points of the stepping cycle were taken as the extreme positions of the metatarsal anthropometric point of the right leg in the sagittal plane. A Qualisys 3D video capture system [Qualisys, Sweden] with a sampling frequency of 500 Hz was used.

Electromyogram (EMG) recordings were made from the muscles of the lower limbs on both sides: the tibialis anterior (TA), medial head of the gastrocnemius (GM), vastus lateralis (VL), biceps femoris (BF), and rectus femoris (RF) muscles. EMG recordings were made using an ME6000 wireless 16-channel biomonitor (Megawin, Finland), with a sampling frequency of 2000 Hz. Disposable cutaneous self-adhesive electrodes with conductive gel and an active contact area of 2.5 cm^2, size 36 × 45 mm (Swaromed, Austria) were used. Electrodes were bipolar. Active electrodes were located in the projections of the motor points of the muscles under study, and reference electrodes were attached along their fibers with an interelectrode distance of 2 cm. EMG recordings were initially filtered with a bandpass filter with a passband of 30–450 Hz and a suppression level of 60 dB with zero delay, and were then averaged over 0.004-sec intervals and re-applied to a 15 Hz low-pass filter using MegaWin software (Megawin, Finland). Figure 1, *a* shows interference EMG samples before and after the preprocessing procedure.

Electroencephalogram (EEG) recordings were made synchronously with EMG recordings, using 11 leads with electrodes located according to the international "10–20" system – O1, O2, P3, P4, C3, C4, F3, F4, T3, T4, and Cz – using an Encephalan-EEGR-19/26 encephalograph recorder (Medicom MTD, Russia). Leads A1 and A2 were used as reference. A helmet of the appropriate size bearing the electrode system was placed on the subject's head. The patient's autonomous unit and most of the cable of the electrode system were placed on the couch next to the subject. Electrode mounting quality was monitored in terms of subelectrode impedance, which was no greater than 10 kΩ. Sampling frequency was 250 Hz and bandwidth was 0.3–70 Hz.

Oculogram and electrocardiogram recordings were made synchronously with the EEG. Additionally, recording electrodes were placed on the vastus lateralis muscle of the right leg and the gastrocnemius muscle to use these signals to suppress artifacts on the EEG. The recorded EEG filtration procedure included an automated method for compensating for artifacts, which consisted of determining the degree of similarity of EEG signals with physiological signals and subtracting them from the EEG with a weighting coefficient. Encephalan-EEG software was used. The Encephalan-EEGR-19/26 was synchronized with other equipment by automatic submission of markers via one of the channels provided in the "Encephalan-EEG" program. Recorded EEG signals with synchronization markers were exported to the Statistica and MATLAB system for further analysis. Figure 1, *b* shows a sample of a native EEG recording and the product of the filtration procedure.

EMG and EEG recordings and anthropometric point coordinates in the 3D system were exported to Statistica

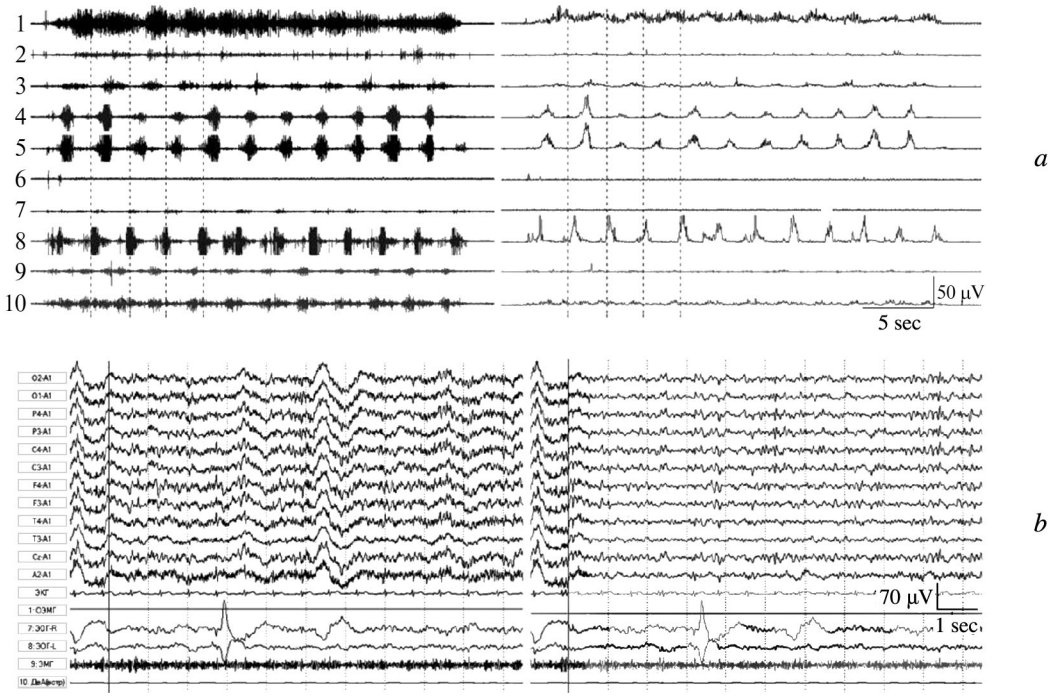

Fig. 1. Samples of skeletal muscle electromyogram (*a*) and electroencephalogram (*b*) recorded during locomotion in conditions of horizontal suspension of the lower limbs. Muscles: 1) TAR, 2) GMR, 3) BFR, 4) RFR, 5) VLR, 6) TAL, 7) GML, 8) BFL, 9) RFL, 10) VLL, where R is the right side and L is the left side. Native recordings are shown at left and traces after processing are shown at right.

(StatSoft, Inc., version 10), where initial data matrixes (X) of dimension ($I \times J$), where I is the number of points (measurements at a time), and J is the number of independent variables (EMG, EEG, etc.), were formed. Additionally, variables were created in the matrixes to identify periods of the stepping cycle and the assignment of data to specific subjects and steps [Moiseev et al., 2022]. All variation series were interpolated relative to a single reference point and standardized to one standard deviation.

Components (synergies) were extracted from matrixes using factor analysis (FA) and principal component analysis (PCA). The original matrix X was decomposed into the product of two matrixes: $X = T \times P + E$, where T is the matrix of counts, P is the matrix of loads, and E is the matrix of residuals. The matrix of loads carries information about relationships between or independence of variables with respect to new formal variables obtained by matrix decomposition, i.e., weighting coefficients; the greater the coefficient, the stronger the connection with the new component. In fact, the value of the coefficient indicates the degree of linearity in changes in the signal, i.e., is a measure of their synchronicity, which is a characteristic feature of synergy. The matrix of counts determines the temporal organization of the identified synergies and represents the projection of the initial data onto the subspace of the main components i.e., activation coefficients. Changes in activation coefficients on the time scale indicate increases or decreases in the activity of the synergy due to synchronous activation of its components.

Matrix decomposition was run in the Statistica environment using the standard modules "Advanced/Multivariate – PCA" and "Mult/Exploratory – Factor." Components with eigenvalues greater than one and accounting for at least 10% of the total variance were considered. The following parameters were analyzed: the number of components extracted (synergies), the percentage of total variance accounted for by each factor in the total dataset (VAF), weighting coefficients, and activation coefficients. At the first stage, synergistic effects at the muscular and cortical levels were extracted and analyzed. The next stage involved multi-level discrete wavelet transformation of EEG signals for each lead, run in the MATLAB system using the "Signal Multiresolution Analyzer" module (MathWorks, USA). As a result, the original signal was represented as eight independent, spatially oriented frequency channels, calculated iteratively [Mallat, 1989]. At each iteration level, signals were thinned after high- and low-pass filtration. The resulting signals were presented in the following frequency ranges [Hz]: 62.5 → 62.5; 30–64.5; 15.5–32; 7.5–16; 3.7–8; 1.8–4; 0.94–2; and 0.1–1 (Fig. 2). The resulting EEG frequency channels for each lead, together with the activation coefficients of three muscle synergies, formed a data matrix in Statistica. Components were extracted from the matrix by PCA. Components including high weighting coefficients of variable muscle synergies (greater than 0.7) were analyzed and compared with wavelet coefficients. This analysis established the degree of synchronization of EEG signals in different frequency ranges with the activation of muscle synergies.

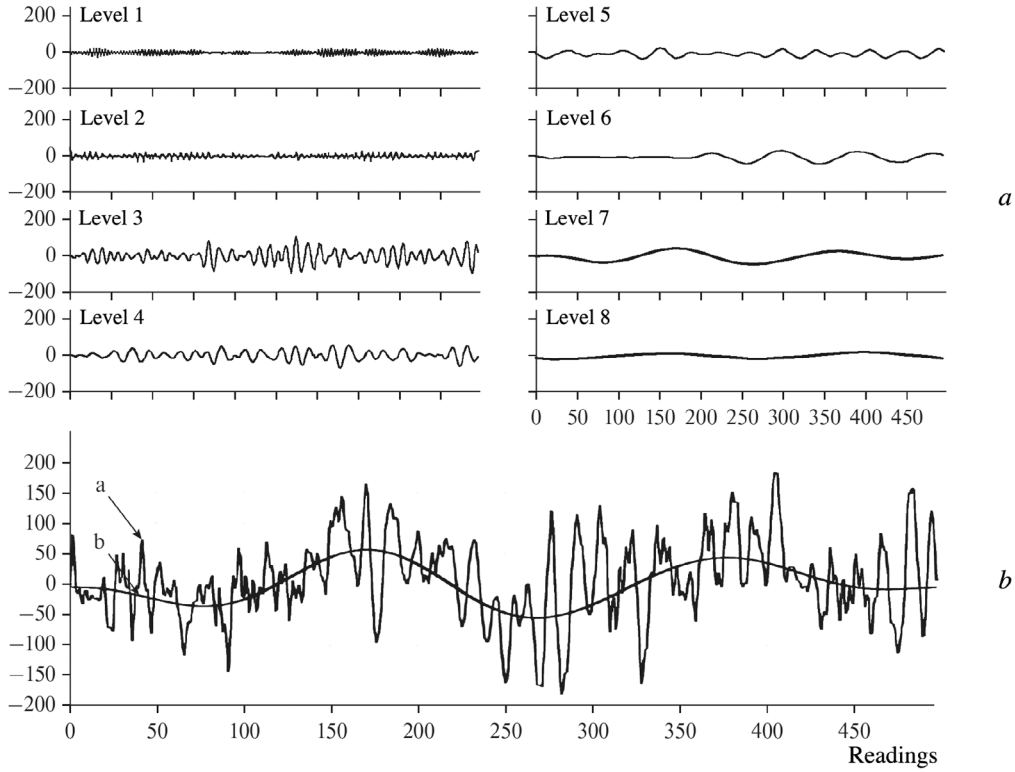

Fig. 2. Discrete wavelet decomposition of a fragment of the EEG signal (lead P4) corresponding to the period of a complete stepping cycle in "horizontal" walking. *a*) Signal decomposition levels (levels 1–8); *b*) original (a) and transformed (b), including decomposition levels 7 and 8, corresponding to the frequency range 0.1–1 Hz.

Mathematical and statistical data processing was run in Statistica 10.0 and included calculation of the arithmetic mean (*M*), the error of the arithmetic mean (*SE*), the standard deviation (*SD*), and the coefficient of variation (*CV*). The activation coefficients of synergies were compared by analysis of the maximum values of cross-correlation functions taking account of offsets relative to zero, where 1 is complete correspondence and 0 is the absence of a relationship. Simple exponential smoothing ($\alpha = 0.01$) was applied to variation series containing synergy activation coefficients before calculating cross-correlation functions.

Results. Decomposition of the matrix with EMG data identified five factors, or synergies, though the last two combined accounted for less than 10% of the explained variance and therefore were not analyzed. It should be noted that use of factor analysis provided a better quality of reconstruction of the original data than the principal components method. The percentage of variance accounted for in the former was $74.00 \pm 0.70\%$, CV = 2.1%, compared with $68.13 \pm 0.69\%$, CV = 12.6% in the latter. The structure of the first motor synergy (MS) was found to include to a greater extent the RF and VL of the right leg; these had the largest weighting coefficients in the first of the factors selected (Fig. 3, *a*). The activation ratios of this synergy showed a temporal pattern with a distinct peak of activity in the second and fourth quarters of the bilateral stepping cycle. The group mean degree of correspondence of the coefficients on multiple implementations of stepping cycles was assessed as high – 0.73 ± 0.03. The second factor included the highest weighting coefficients for the BF of both legs, as well as the GM of the right leg. In the third factor, the GM of the left leg and the RF of the right leg had relatively large weighting coefficients – 0.54 ± 0.04 and 0.51 ± 0.03, respectively. Predominant activation of these muscles, which had the largest weighting coefficients in the structure of the second factor, determined the increase and decrease in the activity of the synergy occurring in the middle and at the end of the stepping cycle. The temporal structure of the third synergy was characterized by periodic bursts of activation at the beginning and end of the stepping cycle, as well as in the second quarter (Fig. 3, *b*).

Decomposition of the matrix with data on the dynamics of electrical activity yielded three components, which together described $81.90 \pm 1.88\%$ of the total variance; low within-group variability in the extraction of components was noted (CV = 7.2%). In this case, the principal components method gave a better result than factor analysis, which accounted for no more than 75% of the total variance in the data. The first identified component was characterized by marked cortical activity in the frontal, central, and parietal leads on the right side. For example, the weighting coefficients in area F4 were 0.84 ± 0.02 and between-individual variability was assessed as low (Fig. 4, *a*). The highest coefficients were found in area Cz – 0.92 ± 0.01. In the left-sided

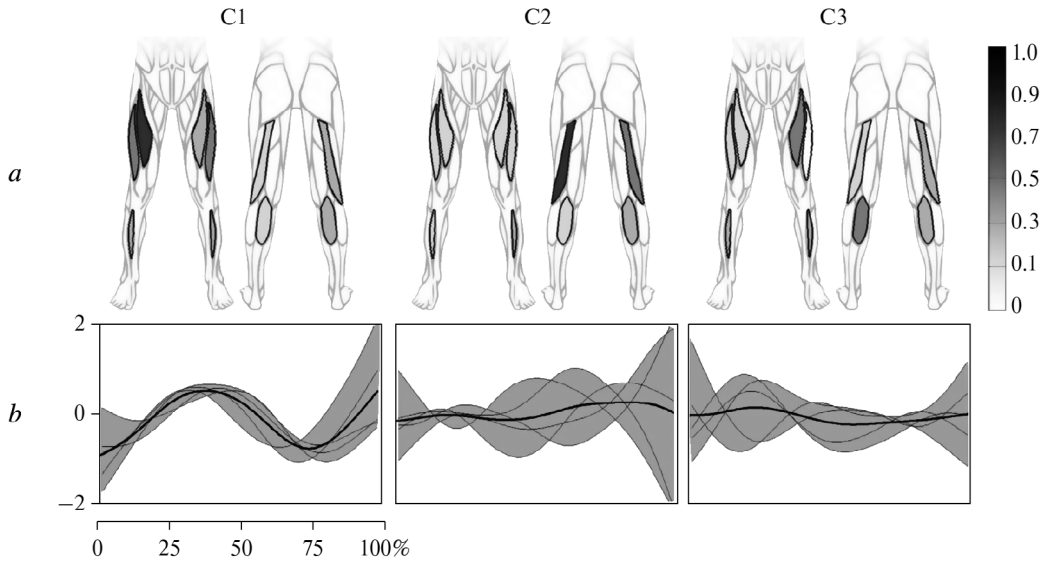

Fig. 3. Weighting coefficients (*a*) and activation coefficients (*b*) of muscle synergies during locomotor activity. In (*b*) the *x* axis shows the stepping cycle and the *y* axis shows values (units). The thick line is the mean within-group pattern; the shading and thin lines show some within-individual patterns. C1, C2, and C3 are extracted components (muscle synergies) 1, 2, and 3, respectively.

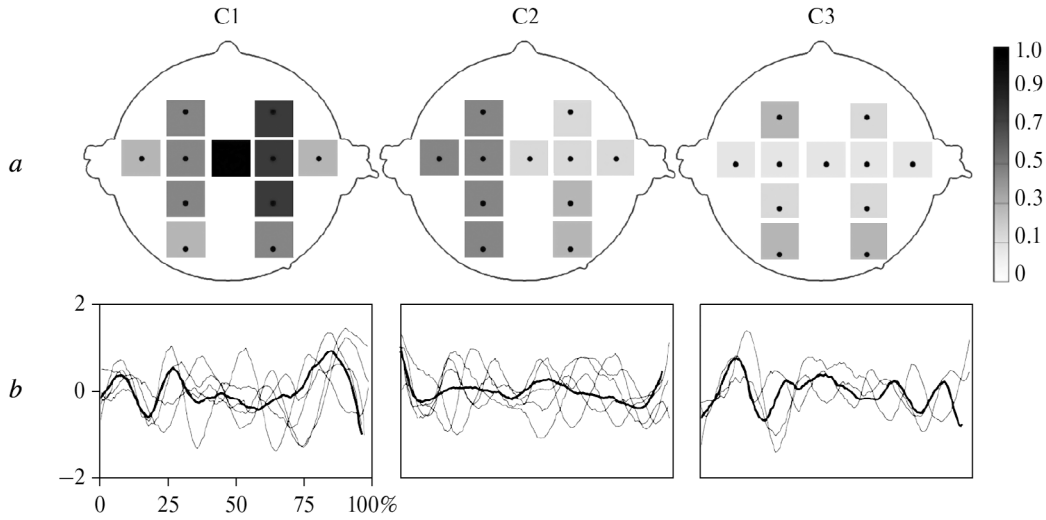

Fig. 4. Weighting coefficients (*a*) and activation coefficients (*b*) of components extracted from EEG activity data on locomotion. C1, C2, and C3 are component numbers. In (*b*) the *x* axis shows the stepping cycle and the *y* axis shows values (units). The thick line is the mean within-group pattern; the shading and thin lines show some within-individual patterns.

leads, average coefficients not exceeding 0.63 ± 0.06 were noted. The activation coefficients of the first component showed three marked peaks – in the first quarter of the locomotor cycle, at the beginning of the second quarter, and in the last quarter. It should be noted that there was high variability in between-individual profiles; the coefficients of cross-correlation functions when comparing these were no greater than 0.27, indicating low correspondence of signals.

The second of the components isolated was characterized by a predominance of activity in the area of the EEG leads on the left side. Thus, the weight coefficients of the leads in the frontal area averaged 0.56 ± 0.04 for the group. The greatest coefficients were obtained in the parietal and central regions – 0.62 ± 0.04 and 0.63 ± 0.04, respectively. In the right-side leads, coefficients were no greater than 0.40 ± 0.03. Activation coefficients in this component showed a decrease in activity at the beginning and an increase at the end of the stepping cycle. Bursts of activity were observed at the transition boundary between the first and second quarters, as well as in the middle of the stepping cycle (Fig. 4, *b*). The coefficients of cross-correlation functions on comparison of between-individual patterns of temporal activation in this component indicated a low correspondence of signals – no more than 0.20 ± 0.03. In the third component, weighting coefficients were predominantly low, not exceeding 0.3. Intermediate coefficients were

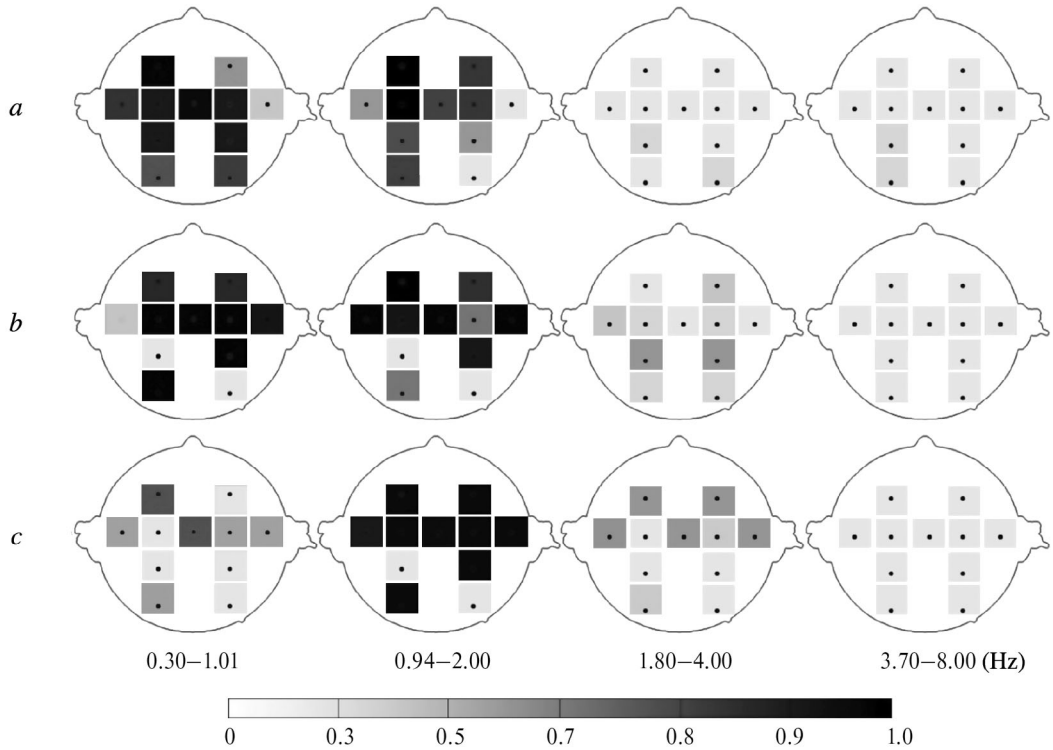

Fig. 5. Weighting coefficients of the first component obtained by decomposition of the matrix including activation coefficients of muscle synergies and wavelets by EEG leads. *a*, *b*, *c*) – muscle synergies 1, 2, and 3.

identified in the occipital leads and left frontal lead. The activation coefficients of the third component showed a peak of activity at the beginning of the stepping cycle and two in its last quarter (Fig. 4, *b*).

In accordance with the study objectives, synchronization of cortical signals in different frequency ranges with the activity of muscle synergies was analyzed. This analysis involved isolating the principal components from a data matrix containing the activation coefficients of the previously identified three muscle synergies and EEG signals in different frequency ranges for each of the leads recorded. Matrix decomposition yielded two components including medium or high weighting coefficients for variables, i.e., EEG leads in different frequency ranges and activation coefficients of muscle synergies, such that the degree of their synchronization could be established. Thus, a high degree of synchronization of EEG activity with the first muscle synergy was found in two frequency ranges (Fig. 5). The highest coefficients in the range of 0.30–1.01 Hz were obtained in the central and parietal, as well as the frontal and mid-temporal regions of the left side. Weighting coefficients here were greater than 0.9. In the range 0.94–2.00 Hz, the highest coefficients were recorded in the frontal region on the left (0.84 ± 0.04) and right (0.93 ± 0.03) sides. Coefficients were large in the central area of both sides, as well as in the left occipital and mid-temporal areas – greater than 0.78. Weighting coefficients in the frequency ranges 1.80–4.00 Hz and 3.70–8.00 Hz were no greater than 0.34. Frequency ranges in which weight coefficients were less than 0.30 were not considered here or further.

A high degree of synchrony was established for the second muscle synergy, mainly in the central and frontal regions. For example, in the frequency range 0.30–1.01 Hz, coefficients in the central areas were 0.92 ± 0.14 and 0.92 ± 0.09, respectively. In the range 0.94–2.00 Hz, synchronization of EEG activity was noted in the central, frontal, and mid-temporal areas (Fig. 5, *b*). In the other frequency ranges considered here, coefficients were no greater than 0.54. Assessment of synchronization of cortical activity with the third muscle synergy revealed high weighting coefficients in the frontal, central, and mid-temporal regions, reaching 0.98 (Fig. 5, *c*).

The second of the components isolated demonstrated high synchronization of cortical activity with muscle synergies, mostly in the range 1.80–4.00 Hz (Fig. 6). In the case of the first muscle synergy, high weighting coefficients were found in the frontal leads – 0.82 ± 0.14 and 0.78 ± 0.09, respectively, as well as the central leads – 0.94 ± 0.04 and 0.96 ± 0.05. The midtemporal cortical areas also demonstrated a high degree of synchrony with muscle synergies – greater than 0.82. High weighting coefficients were also noted in the right parietal (0.96 ± 0.04) and occipital leads (0.94 ± 0.06). In the case of the second muscle synergy, an intermediate degree of synchrony was demonstrated by EEG activity in almost all leads, though this was more marked in the frontal leads – 0.81 ± 0.11 and 0.89 ± 0.09, as well as in the central area on the right side – 0.89 ± 0.04

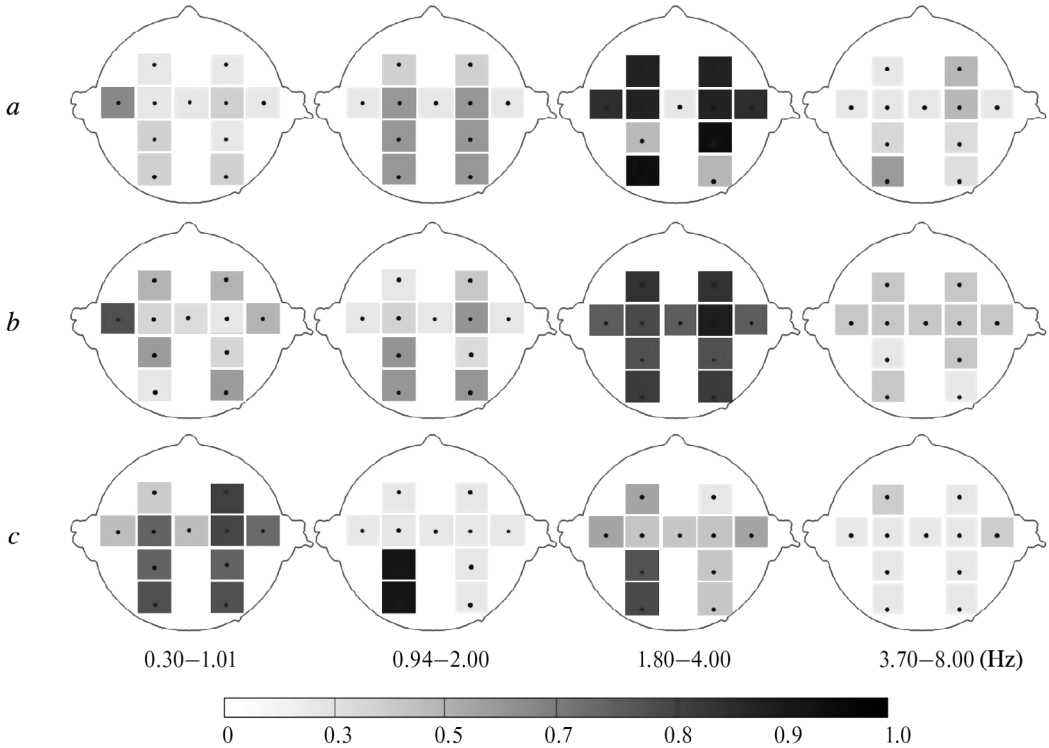

Fig. 6. Weighting coefficients of the second component obtained by decomposition of the matrix including activation coefficients of muscle synergies and wavelets by EEG leads. *a*, *b*, *c*) – muscle synergies 1, 2, and 3.

(Fig. 6, *b*). In the case of the third muscle synergy, high synchrony of EEG signals was noted in the frequency range 0.94–2.00 Hz in the right central and midtemporal leads – greater than 0.92. High weighting coefficients, ranging from 0.72 to 0.84, were also recorded in the frontal lead on the right side, the central, parietal, and occipital leads, and the right midtemporal lead (Fig. 6, *c*).

Discussion. Establishing muscle synergies using data factorization methods is common practice, and three to five are generally identified for locomotion. This number is extracted from almost any set of initial EMG recordings, bilateral or unilateral [Ivanenko et al., 2006; Hug et al., 2010; Santuz et al., 2018]. The time profile of such formations generally has a clear structure which describes most of the variance in EMG data, and has low variability, even when considered on a between-individual basis. The weighting coefficients and vectors of muscle synergies (the composition and ratio of muscle activations within each synergy) turn out to be more variable and depend to a greater extent on the data factorization method used. Our study established five muscle modules using factor analysis. The principal component method was found to be less effective in analysis of MS. The activation coefficients of the first muscle synergy had high reproducibility and clearly distinguishable activation peaks in the second and fourth quarters of the stepping cycle. In most cases, the number of muscles with high weighting coefficients within the modules identified here was no more than two, which is probably explained by the initial set of muscles and the features of the algorithm used to extract components.

The temporal structure of locomotion represented by the activation profiles of the muscles involved in the stepping cycle typically demonstrates fundamental activation profiles determined by the biomechanical structure of locomotion. Such profiles generally have one or two marked peaks occurring during those periods of the stepping cycle in which greater muscle effort is required, such as when movements change direction [DeMarchis et al., 2015]. In this regard, our results are consistent with published data. We note that the peaks of MS activity occurred during periods in which lower limb movements change direction, i.e., in the extreme positions of the metatarsal anthropometric points with maximum separation of the feet. Predominant activation of muscles that form the stereotypical locomotor pattern was also noted. For example, the BF and VL of the right lower limb had high weighting coefficients in the first MS, and their activation was comparable in time to hip flexion occurring in the first and second quarter of the stepping cycle. The activation coefficients of the first synergy in this same time period indicated an increase in the activity of the synergy (a peak of activation was noted).

Assessment of the contributions of skeletal muscle activity to a synergy generally reveals some differences on execution of similar motor tasks in different conditions, such as walking on a treadmill and on the floor, walking in non-standard conditions, while immersed in water, etc. [Santuz et al.,

2018; Mileti et al., 2020; Mehryar et al., 2020; Yokoyama et al., 2021; Saito et al., 2021]. These differences are partly due to the use of different methods for extracting synergies, as well as the particular set of source EMG recordings used in the analysis. Pre-processing of the electromyogram is also of great importance, as different filtration parameters affect the quality of data reconstruction. In addition to computational aspects, the different compositions of muscle synergies, as determined by the weighting coefficients in the structure of the extracted components, may be due to the use of different tactics for constructing movements in the central nervous system [Gelfand et al., 1962].

The concept of synergy suggests that the number of control modules should, on a priori grounds, be smaller than the number of controlled modules, and their total number may reflect the complexity of the control system. The approach based on isolating components using data factorization methods to study cortical activity is not new. Attempts have been made to assess synchronization of neuron activity in remote parts of the cerebral cortex [Overduin et al., 2015; Yoshimura et al., 2017]. Independent component analysis was used to separate EEG signals into independent sources demonstrating synchronization of activity in different areas of the brain during walking on level and inclined surfaces [Bradford et al., 2016]. It should be noted that, regardless of the number of leads used, decomposition of EEG signals into components identifies no more than three components, and this is true for both discrete and cyclic movements.

We identified two components, the first of which predominantly included activity in the frontal, central, and parietal areas of the cortex on the right side, the second being characterized by synchronization of cortical activity in leads on the left side, where the largest weighting coefficients were obtained. One of the properties of the principal components method is orthogonality, i.e., independence of the principal components, such that the component structure may point to different and independent processes. In our case, synchronization of activity in different areas of the cortex on the left (component 1) and right (component 2) sides is probably associated with alternating activation of the flexor and extensor muscles of the contralateral limb during locomotion. This can easily be observed on the EMG by analyzing the burst activity of, for example, the biceps femoris muscle of the right leg and the rectus femoris muscle of the left leg. Similar results were described using analysis of coherence between the motor cortex and muscle groups of the contralateral limb [Zandvoort et al., 2019]. A rhythmic increase in EEG spectral power in the left and right hemispheres associated with alternating activation of locomotor muscles has also been demonstrated [Roeder et al., 2018; Bourguignon et al., 2019].

We captured data indicating synchronization of activity in various areas of the cortex on both sides. These patterns are probably due to the specific characteristics of performing locomotion in conditions of gravitational unloading and the associated features of receptor signaling. Thus, there is virtually no afferentation from the supporting zones of the foot in horizontal suspension. Perception of body movement in space based on signals from the receptors of the vestibular apparatus and the visual and auditory analyzers is absent or distorted. This creates a specific set of afferent signals from different receptors which is different from the set occurring in natural walking in an upright position. Thus, not only the motor part of the cortex, but also the associative, visual, and sensorimotor areas, may be involved in the processing of such information.

Coherence analysis is a widely used method for assessing cortico-muscular interaction and reflects the phenomenon of synchronicity in the frequency domain [Kulaichev, 2009]. Our work did not use coherence analysis as such. We addressed the relationship between wavelet-transformed EEG signals (wavelets) and parameters of the temporal structure (activation coefficients) of muscle synergies. In essence, this is a comparison and search for synchronicity in the time domain rather than the frequency domain, even taking account of the fact that the initial signals were EEG time series presented in different frequency ranges. Results assessed in the coherence paradigm may therefore differ from those obtained by other methods (or a combination of methods), as they represent different processes implemented in the frequency and time domains. In addition, some hold the view that analysis of signal coherence does not support direct identification of the central control signal to the muscles or, conversely, the sensorimotor signal from the periphery to the brain, but is only a measure of synchrony [Kurganskaya et al., 2020; Yang et al., 2018]. Studies using spectral analysis of EMG signals demonstrated high levels of between-muscle coherence in the low-frequency ranges (0–5 Hz, 5–20 Hz) during postural tasks [Danna-Dos-Santos et al., 2015]. The finding of significant between-muscle coherence in the α, β, and γ bands during walking led to the conclusion that coordination of the upper and lower limbs shares common cortical mechanisms [Weersink et al., 2021]. The high level of coherence of EMG signals detected in the same main cortical activity frequency ranges during locomotion and on execution of postural tasks can be seen as evidence of the central control of muscle activity via synchronization of cortical signals and the activity of spinal motoneurons [Mima et al., 1999]. Coherence analysis results identified slow cortical cyclic activity, similar to that generated by spinal generators during locomotion [Hall et al., 2014].

Our studies demonstrated synchronization of the activity of several cortical areas and identified muscle synergies, mainly in three frequency ranges: 0.30–1.01, 0.94–2.00, and 1.80–4.00 Hz. As noted earlier, the components isolated by factorization methods reflect independently occurring processes, so our data showing spatiotemporal structuring of cortical activity may indicate cortical control of muscle synergies in two ways. The first involves the control of two

muscle synergies, synchronizing the activity of multiple cortical areas in the frequency range 0.30–2.00 Hz. The second involves controlling two synergies in the range 1.80–4.00 Hz and one in the range 0.30–1.01 Hz. Synchronization of cortical activity with muscle synergies in other frequency ranges is essentially not observed.

Despite the fact that low-frequency cortical activity is traditionally correlated with the state of deep sleep, a number of studies have obtained results showing increases in cortical activity in the δ range (0.2–4 Hz) in the central frontal, central, and parietal areas in association with changes in the sensory and postural conditions of motor task performance [Ozdemir et al., 2017]. A large contribution of EEG δ rhythms to the regulation of muscle activity has been noted [Nakanishi et al., 2013, 2014]. Electrocorticographic studies in experiments on primates allowed movement intention (trajectory of hand movement) to be classified, with the frequency bands 1.5–4 and 50–90 Hz making the greatest contributions to decoding of EEG signals [Shin et al., 2012]. Locomotor muscle activation during treadmill walking correlated with slow cortical waves, with decoding accuracy being higher for muscle groups than for individual muscles [Yokoyama et al., 2019]. Thus, there are grounds for the view that low-frequency cortical signals may be directly related to the control of muscle synergies.

In addition, it is known that two independent mechanisms can be used to control cyclic activity. The first determines the ratios of muscles and muscle groups (which may be synergies) involved in movement, i.e., is a pattern-forming mechanism; the second takes part in forming the sequence of muscle activations and determines the temporal structure of the locomotor cycle, i.e., is a rhythm-generating mechanism [Churchland et al., 2012; Hogan and Sternad, 2007]. The activation and weighting coefficients of muscle synergies obtained by decomposition of matrixes by factorization methods may reflect the operation of these mechanisms. Despite the fact that these mechanisms were considered at the spinal level, it is likely that they may be involved at other levels of the central nervous system, including the cortical level. Thus, the rhythm-generating mechanism may ensure synchronization of cortical rhythms and the neural networks of the spinal cord. In this case, the combined change in signals recorded at different levels of the central nervous system may be a reflection of centralized control.

Conclusions. Control of movement structure in conditions of horizontal suspension of the lower limbs is realized mainly through three muscle synergies. Their spatiotemporal structures display fundamental activation profiles determined by the biomechanical structure of locomotion in these conditions.

Synchronization of the activity of the motor, associative, visual, and sensorimotor areas of the cortex on both sides is due to the specific characteristics of locomotion in conditions of gravitational unloading and the associated features of receptor signaling. The components identified, which point to synchronization of different areas of the cortex on the right and left sides, may reflect control processes associated with driving alternating activation of the flexor and extensor muscles of the contralateral limb in the process of locomotion.

Data on the spatiotemporal structuring of cortical activity indicate separate control of muscle synergies via synchronization of cortical commands and the temporal organization of muscle synergies in frequency ranges from 0.30 Hz to 8.00 Hz. Such patterns may reflect the operation of a rhythm-generating mechanism involved in controlling cyclic activity.

REFERENCES

Amundsen Huffmaster, S. L., Van Acker, G. M., 3rd, Luchies, C. W., and Cheney, P. D., "Muscle synergies obtained from comprehensive mapping of the primary motor cortex forelimb representation using high-frequency, long-duration ICMS," *J. Neurophysiol.*, **118**, No. 1, 455–470 (2017).

Bernshtein, N. A., *The Physiology of Movement and Activity*, Nauka, Moscow (1990).

Bourguignon, M., Jousmäki, V., Dalal, S. S., et al., "Coupling between human brain activity and body movements: Insights from non-invasive electromagnetic recordings," *NeuroImage*, **203**, 116177 (2019).

Bradford, J. C., Lukos, J. R., and Ferris, D. P., "Electrocortical activity distinguishes between uphill and level walking in humans," *J. Neurophysiol.*, **115**, No. 2, 958–966 (2016).

Churchland, M. M., Cunningham, J. P., Kaufman, M. T., et al., "Neural population dynamics during reaching," *Nature*, **487**, No. 7405, 51–6 (2012).

Danna-Dos-Santos, A., Degani, A. M., and Boonstra, T. W., "The influence of visual information on multi-muscle control during quiet stance: a spectral analysis approach," *Exp. Brain Res.*, **233**, No. 2, 657–669 (2015).

De Marchis, C., Severini, G., Castronovo, A. M., et al., "Intermuscular coherence contributions in synergistic muscles during pedaling," *Exp. Brain Res.*, **233**, No. 6, 1907–19 (2015).

De Vries, I. E., Daffertshofer, A., Stegeman, D. F., and Boonstra, T. W., "Functional connectivity in the neuromuscular system underlying bimanual coordination," *J. Neurophysiol.*, **116**, No. 6, 2576–2585 (2016).

Frère, J., "Spectral properties of multiple myoelectric signals: New insights into the neural origin of muscle synergies," *Neuroscience*, **355**, 22–35 (2017).

Gel'fand, I. and Tsetlin, M., "Some ways of controlling complex systems," *UMN*, **17**, No. 1, 3–25 (1962).

Gerasimenko, Y. P., Lu, D. C., Modaber, M., et al., "Noninvasive reactivation of motor descending control after paralysis," *J. Neurotrauma*, **32**, No. 24, 1968–80 (2015).

Gorodnichev, R. M., Pivovarova, E. A., Puhov, A., et al., "Transcutaneous electrical stimulation of the spinal cord: a noninvasive tool for the activation of stepping pattern generators in humans," *Hum. Physiol.*, **38**, No. 2, 158–167 (2012).

Grigor'ev, A. I., Kozlovskaya, I. B., and Shenkman, B. S., "The role of supporting afferentation in the organization of the tonic muscular system," *Ros. Fiziol. Zh.*, **90**, No. 5, 507–521 (2004).

Gurfinkel', V. S., Levik, Yu. S., Kazennikov, O. V., and Selionov, V. A., "Do humans have a stepping generator?" *Fiziol. Cheloveka*, **24**, No. 3, 42–50 (1998).

Hall, T. M., de Carvalho, F., and Jackson, A., "A common structure underlies low-frequency cortical dynamics in movement, sleep, and sedation," *Neuron*, **83**, No. 5, 1185–99 (2014).

Hogan, N. and Sternad, D., "On rhythmic and discrete movements: reflections, definitions and implications for motor control," *Exp. Brain Res.*, **181**, No. 1, 13–30 (2007).

Hug, F., Turpin, N. A., Couturier, A., and Dorel, S., "Consistency of muscle synergies during pedaling across different mechanical constraints," *J. Neurophysiol.*, **106**, No. 1, 91–103 (2011).

Ivanenko, Y. P., Poppele, R. E., and Lacquaniti, F., "Motor control programs and walking," *Neuroscientist*, **12**, No. 4, 339–48 (2006).

Kulaichev, A. P., "The informativeness of coherence analysis in EEG studies," *Zh. Vyssh. Nerv. Deyat.*, **59**, No. 6, 757–767 (2009).

Kurganskaya, M. E., Bobrov, P. D., Frolov, A. A., and Semenova, E. I., "Corticomuscular interaction during real and imaginary movements of the hand," *Zh. Vyssh. Nerv. Deyat.*, **70**, No. 6, 738–751 (2020).

Latash, M., "Motor synergies and the equilibrium-point hypothesis," *Motor Control*, **14**, No. 3, 294–322 (2010).

Mallat, S. G., "A theory for multiresolution signal decomposition: the wavelet representation," *IEEE Trans. Pattern Analysis Machine Intell.*, **11**, No. 7, 674–693 (1989).

Mehryar, P., Shourijeh, M., Rezaeian, T., et al., "Differences in muscle synergies between healthy subjects and transfemoral amputees during normal transient-state walking speed," *Gait Posture*, **76**, 98–103 (2020).

Mileti, I., Serra, A., Wolf, N., et al., "Muscle activation patterns are more constrained and regular in treadmill than in overground human locomotion," *Front. Bioeng. Biotechnol.*, **8**, 581619 (2020).

Mima, T. and Hallett, M., "Corticomuscular coherence: a review," *J. Clin. Neurophysiol.*, **16**, No. 6, 501–511 (1999).

Moiseev, S. A., "Spatiotemporal patterns of intermuscular interaction during locomotion induced by transcutaneous electrical stimulation of the spinal cord," *Zh. Evolyuts. Biokhim. Fiziol.*, **58**, No. 6, 94–102 (2022).

Moiseev, S., Pukhov, A., Mikhailova, E., and Gorodnichev, R., "Methodological and computational aspects of extracting extensive muscle synergies in moderate-intensity locomotions," *J. Evol. Biochem. Phys.*, **58**, 88–97 (2022).

Nakanishi, Y., Yanagisawa, T., Shin, D., et al., "Decoding fingertip trajectory from electrocorticographic signals in humans," *Neurosci. Res.*, **85**, 20–7 (2014).

Nakanishi, Y., Yanagisawa, T., Shin, D., et al., "Prediction of three-dimensional arm trajectories based on ECoG signals recorded from human sensorimotor cortex," *PLoS One*, **8**, No. 8, e72085 (2013).

Overduin, S. A., d'Avella, A., Roh, J., et al., "Representation of muscle synergies in the primate brain," *J. Neurosci.*, **35**, No. 37, 12615–24 (2015).

Ozdemir, R. A., Contreras-Vidal, J. L., and Paloski, W. H., "Cortical control of upright stance in elderly," *Mech. Aging Dev.*, **169**, 19–31 (2018).

Pei, D., Olikkal, P., Adali, T., and Vinjamuri, R., "Reconstructing synergy-based hand grasp kinematics from electroencephalographic signals," *Sensors (Basel)*, **22**, No. 14, 5349 (2022).

Reyes, A., Laine, C. M., Kutch, J. J., and Valero-Cuevas, F. J., "Beta band corticomuscular drive reflects muscle coordination strategies," *Front. Comput. Neurosci.*, **11**, 17 (2017).

Roeder, L., Boonstra, T. W., Smith, S. S., and Kerr, G. K., "Dynamics of corticospinal motor control during overground and treadmill walking in humans," *J. Neurophysiol.*, **120**, No. 3, 1017–1031 (2018).

Saito, H., Yokoyama H, Sasaki, A., et al., "Flexible recruitments of fundamental muscle synergies in the trunk and lower limbs for highly variable movements and postures," *Sensors (Basel)*, **21**, No. 18, 6186 (2021).

Santuz, A., Ekizos, A., Janshen, L., et al., "Modular control of human movement during running: An open access data set," *Front. Physiol.*, **9**, 1509 (2018).

Shin, D., Watanabe, H., Kambara, H., et al., "Prediction of muscle activities from electrocorticograms in primary motor cortex of primates," *PLoS One*, **7**, No. 10, e47992 (2012).

Weersink, J. B., de Jong, B. M., Halliday, D. M., and Maurits, N. M., "Intermuscular coherence analysis in older adults reveals that gait-related arm swing drives lower limb muscles via subcortical and cortical pathways," *J. Physiol.*, **599**, No. 8, 2283–2298 (2021).

Yang, Y., Dewald, J., Van der Helm, F., and Schouten, A. C., "Unveiling neural coupling within the sensorimotor system: directionality and nonlinearity," *Eur. J. Neurosci.*, **48**, No. 7, 2407–2415 (2018).

Yarossi, M., Brooks, D. H., Erdoğmuş, D., and Tunik, E., "Similarity of hand muscle synergies elicited by transcranial magnetic stimulation and those found during voluntary movement," *J. Neurophysiol.*, **128**, No. 4, 994–1010 (2022).

Yokoyama, H., Kaneko, N., Ogawa, T., et al., "Cortical correlates of locomotor muscle synergy activation in humans: An electroencephalographic decoding study," *iScience*, **15**, 623–639 (2019).

Yokoyama, H., Kato, T., Kaneko, N., et al., "Basic locomotor muscle synergies used in land walking are finely tuned during underwater walking," *Sci. Rep.*, **11**, No. 1, 18480 (2021).

Yoshimura, N., Tsuda, H., Kawase, T., et al., "Decoding finger movement in humans using synergy of EEG cortical current signals," *Sci. Rep.*, **7**, No. 1, 11382 (2017).

Zandvoort, C. S., Van Dieën, J. H., Dominici, N., and Daffertshofer, A., "The human sensorimotor cortex fosters muscle synergies through cortico-synergy coherence," *NeuroImage*, **199**, 30–37 (2019).